Nematodynamics modelling under extreme mechanical and electric stresses

2015 J. Phys.: Conf. Ser. 574 012102

(http://iopscience.iop.org/1742-6596/574/1/012102)

Nematodynamics modelling under extreme mechanical and electric stresses

Antonino Amoddeo

Department of Civil, Energy, Environmental and Materials Engineering Università "Mediterranea" di Reggio Calabria Via Graziella 1, Feo di Vito, I-89122 Reggio Calabria, Italy

E-mail: antonino.amoddeo@unirc.it

Abstract. Nematic liquid crystals confined in asymmetric π-cells and subjected to intense electrical and mechanical stresses undergo strong distortions which can be relaxed by means of the order reconstruction, a fast switching mechanism connecting topologically different textures, assuming bulk and/or surface characteristics depending on both amplitude of the applied electric fields and anchoring angles of the nematic molecules on the confining surfaces. In the frame of the Landau-de Gennes order tensor theory, we provide a numerical model implemented with a moving mesh finite element method appropriate to describe the nematic order dynamics, allowing to map the switching properties of the nematic texture.

1. Introduction

Thermotropic nematic liquid crystals (NLC) are elongated molecules which exhibit orientational order, schematically represented as rods having cylindrical symmetry. In most electro-optical phenomena, the average orientation of the NLC long axis can be described by a dimensionless unit vector, the director $\boldsymbol{n}$, while the degree of order along such direction is accounted for by the scalar order parameter S: as NLCs possess a unique optical axis and cylindrical symmetry, they are said uniaxial [1]. Applying to a nematic texture distortions over length scales comparable to the biaxial coherence length ξ_b [2], the uniaxial symmetry is broken and the system presents two distinct optical axes. As a consequence, local biaxial domains grow, lowering the degree of order, and bistable behaviours become possible. Such phenomena attract great attention due to their direct influence on the optical an switching properties of NLC, but in this case the description requires the coupling of the $\boldsymbol{n}$ and S parameters within the Landau-de Gennes theory based on the order tensor $\mathbf{Q}$ [1].

In a π-cell a thin film of nematic material is confined between two flat glass plates, which internal faces are treated so as to align the nematics on both surfaces with strong anchoring energy and a pretilt angle θ: the two plates are arranged in an anti-parallel configuration generating a splayed texture [2], a set-up admitting the existence of a second topologically distinct texture where the nematic is π-twisted (or π-bent), and the energy barrier between them prevents any spontaneous relaxation from each other. Applying an electric field perpendicularly to the boundary plates the initial splay texture can be switched into the topological different bend one by means of the biaxial order reconstruction, by which the local order of the nematic phase is changed without any macroscopic director rotation.

Recently, using the Finite Element Method (FEM), we implemented the Moving Mesh Partial Differential Equation (MMPDE) numerical technique [3-6], in order to solve the Partial Differential

Equations (PDEs) system arising from the modelling of the order dynamics inside a π-cell containing a 5CB NLC. In such technique, the grid points in which the simulated domain is discretized are moved according to a monitor parameter towards regions where the gradient of the order, $\nabla\mathbf{Q}$, is growing: keeping constant the nodal connectivity and the number of mesh points inside the domain, the latter are clustered into regions of high spatial variability where more detail is required, thus improving the resolution; further, being the domain regions where $\nabla\mathbf{Q}$ is growing *apriori* unknown, a constant number of nodes allows computational saving, since a smaller number of mesh points is needed with respect to simulations performed on uniform grids. We present a numerical investigation of the biaxial order dynamics of a 5CB NLC confined in a asymmetric π-cell performed using the MMPDE technique in order to solve the time-dependent **Q** tensor governing equations, monitoring the evolution of both biaxiality and **Q**-eigenvalues, for applied electric fields with amplitudes extending far above the threshold value required to induce order reconstruction transitions in the bulk [2], imposing variable degrees of asymmetry.

2. Model and method

In the frame of the Landau-de Gennes theory, orientation and order of biaxial nematics are globally described by the symmetric, second-rank, traceless tensor in the orthonormal basis of its eigenvectors $\{\boldsymbol{e}_1, \boldsymbol{e}_2, \boldsymbol{e}_3\}$ [1,7]

$$\mathbf{Q} = \sum_{\boldsymbol{i}=1}^{3} s_{\boldsymbol{i}} \boldsymbol{e}_{\boldsymbol{i}} \otimes \boldsymbol{e}_{\boldsymbol{i}} \tag{1}$$

where the $\boldsymbol{e}_i$ lie along the directions of the preferred molecular orientation, and are assumed as pointing along the x, y and z direction of the laboratory frame of reference, respectively; the associated eigenvalues, s_i, represent the degree of order along such directions, and the isotropic, uniaxial or biaxial phases of nematics can be distinguished considering the s_i. When all the three eigenvalues vanish the calamitic molecules are in the isotropic phase, and the optical behaviour of the material is as an ordinary isotropic fluid; the uniaxial nematic phase presents a unique optical axis, described by the eigenvector $\boldsymbol{e}_i=\boldsymbol{n}$ associated to the maximum eigenvalue s_{max} giving the scalar order parameter $S=(3/2)s_{max}$, while in the biaxial nematic phase, all the eigenvalues are different.

The **Q** dynamical evolution model requires the minimization of the free energy density functional $\boldsymbol{F}$ inside the cell containing the NLC [1], which contributions are assumed to originate from bulk only, since surface terms are neglected because of the fixed boundary conditions imposed, thus leading to infinite anchoring strength. Neglecting ion effects [2] and assuming small **Q** distortions, thermotropic, elastic and electric contributions, respectively F_t, F_d and F_e, can be expressed in powers of **Q**

$$\boldsymbol{F} = \int_V \left(F_t + F_d + F_e\right) dV \tag{2}$$

The balance between the dissipation function D and the free energy variation [8,9] gives the generalized Euler-Lagrange equation (3), where the subscript "$_j$" denotes differentiation with respect to the spatial coordinates x_1, x_2 and x_3, summation over repeated indices is assumed, and the order tensor is expressed in terms of the independent parameters q_i, $i\in[1,5]$,

$$\frac{\partial D}{\partial \dot{q}_i} + \frac{\partial F_t}{\partial q_i} + \frac{\partial F_e}{\partial q_i} + \frac{\partial F_d}{\partial q_i} - \frac{\partial}{\partial x_j}\left(\frac{\partial F_d}{\partial q_{i,j}}\right) - \frac{\partial}{\partial x_j}\left(\frac{\partial F_e}{\partial q_{i,j}}\right) = 0, \qquad i=1\ldots5 \tag{3}$$

The PDEs system (3), together with the governing equation for the electric potential U

$$\nabla\cdot\boldsymbol{D} = \nabla\cdot\left(-\varepsilon_0\boldsymbol{\varepsilon}\nabla U + \boldsymbol{P}_S\right) = 0 \tag{4}$$

where $\boldsymbol{D}$, ε_0, $\boldsymbol{\varepsilon}$ and $\boldsymbol{P}_S$ are, respectively, the displacement field, the vacuum dielectric permeability, the dielectric tensor and the spontaneous polarization vector, represent a system of six coupled PDEs solved imposing Dirichlet boundary conditions on the boundary surfaces of the π-cell, giving the dynamical evolution of the system. Full details about model and development can be found in [3-6]. The degree of biaxiality can be obtained from its invariant measure [2]

$$\beta^2 = 1 - 6\frac{tr\left(\mathbf{Q}^3\right)^2}{tr\left(\mathbf{Q}^2\right)^3} \in [0,1] \tag{5}$$

considering that a uniaxial nematic texture has β^2=0, while the maximum of biaxiality, β^2=1, corresponds to a biaxial nematic phase.

Starting from the discretization of the one dimensional integration domain, equidistributing in each subinterval an appropriate monitor function, a functional which can depend on the gradient of the unknown solution or on the solution error, a quality control on the mesh map is attained, resulting in a quite efficient method capable of accurate representations of sharp solution features. Denoting *u(z,t)* a solution of a system PDEs over a physical domain Ω_p = [0,1] with *z* physical coordinate, if ξ is a computational coordinate of a fixed computational domain Ω_c = [0,1], we define a one-to-one mapping from physical space $\Omega_p \times (0,T]$ to computational space $\Omega_c \times (0,T]$ as $\xi = \xi(z,t)$, $z \in \Omega_p$, $t \in (0,T]$, and its reverse from computational space $\Omega_c \times (0,T]$ to physical space $\Omega_p \times (0,T]$ as $z = z(\xi,t)$, $\xi \in \Omega_c$, $t \in (0,T]$. The equidistribution of the monitor function *M(u(z,t))* over the one-dimensional domain gives the mesh equation in differential form [3,4],

$$M(z(x,t))\frac{\partial}{\partial \xi} z(x,t) = \int_0^1 M(u(s,t))\,ds = C(t) \tag{6}$$

and we have demonstrated [4] that the choice of the monitor function tested by Beckett et al. [10], ensures a good quality control of the meshes and final convergence of the FEM solution. Hence we put

$$M(u(z,t)) = \int_0^1 \left(\left|\frac{\partial u(z,t)}{\partial z}\right|\right)^{1/2} dz + \left(\left|\frac{\partial u(z,t)}{\partial z}\right|\right)^{1/2}, \tag{7}$$

having the advantages of being naturally smoothed, with no need for external interventions.

The FEM discretization of the multidimensional time-dependent problem is done via the method of lines, while the adaptive solution process involves (i) a mesh generation using the equidistribution principle based on the numerical solution at the current time step and (ii) the PDEs solution on the new generated grid and then updated in time.

The PDEs solution was carried out replacing in (7) the unknown *u(z,t)* with $tr(\mathbf{Q}^2)$, a quantity which is rapidly varying when the degree of order is not constant. At t=0 s a rectangular electric pulse is applied perpendicularly to the plates for a duration Δt = 0.25 ms. The imposed pretilt angles, both measured with respect to the plates are, on the lower boundary surface θ_L = 19°, while on the upper boundary plate θ_U was in the [-19°,0°] range with steps variable from 0.1° to 1° as needed. The investigated amplitudes of the applied electric pulse E ranged from 15 V/μm up to 90 V/μm, with steps variable from 1 to 5 V/μm. The dynamical evolution of the **Q** tensor inside the cell was sampled with a time step size δt= 0.1 μs, using the physical parameters typical for 5CB NLC at ΔT=-1°C [2], discretizing the physical domain with a mesh of 285 grid points.

3. Results and discussion

It has been demonstrated [3], that the switching properties of NLCs confined in a π-cell depend on both E and θ_U, once fixed θ_L. To build a phase diagram of the nematic switching regime, monitoring the biaxiality arising in the cell over several points of the (E, θ_U) plane is required. The results of the

biaxiality computations extended to a wide range of (E, θ_U) pairs are summarized in the phase diagram of figure 1, where the boundaries among bulk switching (BS), surface switching (SS), bulk plus surface switching (BSS) or no switching (NS) regimes,

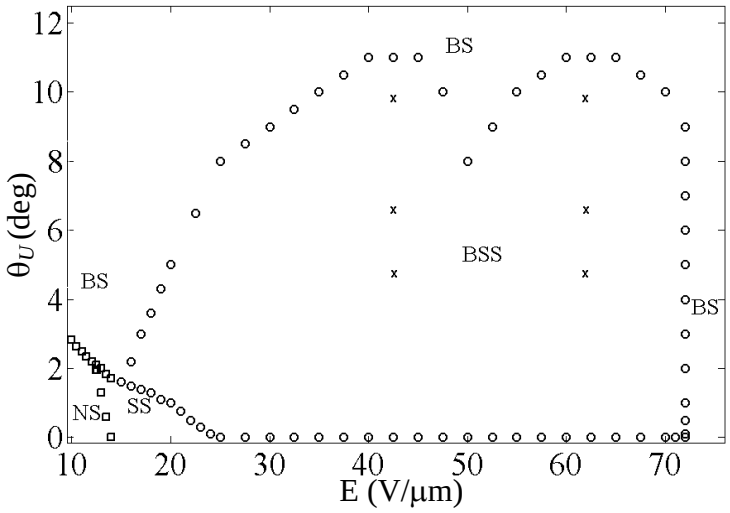

Figure 1. Phase diagram of the biaxial order reconstruction for θ_L = 19°: on the horizontal axis are reported the applied electric pulse amplitudes E, and on the vertical axis are represented the opposite of the anchoring angles θ_U.

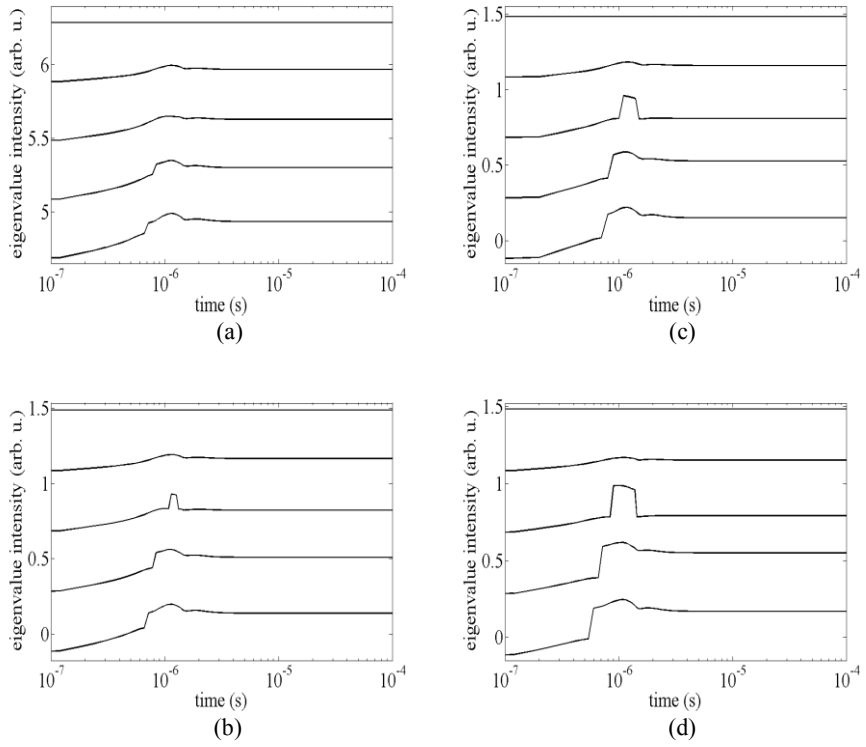

Figure 2. Temporal evolution of the s_3 eigenvalue computed on the first five mesh point starting from the upper boundary surface (top curve), obtained applying a pulse with amplitude E=42.5 V/μm, for θ_U values of -4° (a), -6° (b), -9.5° (c) and -14° (d), where on the horizontal axis time is reported in logarithmic scale.

obtained imposing θ_L = 19°, are indicated by circles. Each point in the (E, θ_U) plane corresponds to a computed biaxiality map (see [3]), for which we read off and referred the corresponding texture as obeying to one of the above switching mechanisms. The points obtained for 10 V/μm ≤ E ≤ 14 V/μm and 0° ≤ θ_U ≤ 3°, represented as squares, well reproduce that presented in [3]. It results a partition of the (E, θ_U) plane in four regions, in each of that are mapped textures homogeneous as regards their switching regime. A large portion of the phase diagram concerns the coexistence of both surface and

bulk order reconstruction transitions, delimited by a bi-lobed boundary, and above E=70 V/μm, whatever θ_U is, the surface transition disappears: hence we expect that, for (E,θ_U) pairs falling in each of the lobed region of the phase diagram, the relaxation mechanism of the nematic texture switches over differently, along the cell thickness. In figure 1, with "**x**" are marked (E, θ_U) pairs for which we monitored the temporal evolution of the s_3 eigenvalue, as it is very sensitive to order variations along the electric field direction [6], i.e. the z-direction, adding also (E=42.5 V/μm, θ_U =-14°) and (E=62 V/μm, θ_U =-14°), not shown for scale reasons. The results obtained applying a pulse with amplitude E=42.5 V/μm are shown in figure 2. As the nematic molecules adsorbed on the confining plate are fixed by the infinite anchoring energy, the degree of order along $\boldsymbol{e_3}$ does not change and s_3 remain constant on the upper plate, for each of the anchoring angles. For θ_U =-4°, figure 2(a), during the time evolution s_3 increase smoothly on the first two grid points below the upper boundary plate, second and third curve from the top, a behaviour typical of second order transitions characterizing biaxial phenomena, in which the strong distortion relaxes through a wealth of biaxial states without any director rotation [6]; on the fourth grid point, instead, the discontinuity marks a first order transition, as the director $\boldsymbol{n}$ reorients along the z-direction under the effect of the applied electric pulse, then a predominant uniaxial order establishes. Imposing θ_U =-6°, figure 2(b), the temporal evolution of s_3 on the second grid point below the surface shows a sharp structure superimposed over the smooth evolution: the nematic director starts to reorient but it is suddenly pulled back, denoting a dynamical evolution of the biaxiality mediated by a metastable uniaxial state; on the remaining two points the s_3 evolution shows a first order transition. Increasing θ_U up to -14°, the duration of the metastable state increases and all the features become sharper and faster, see figures 2(c)-2(d). For E=62 V/μm, on going from θ_U =-4°to θ_U =-14°, in the s_3 temporal evolution the metastable uniaxial state is not present, and a stable director reorientation occurs on going from the upper boundary surface towards the bulk; the relative evolution is not shown for space reasons.

4. Conclusions

Our technique allowed us to map a phase diagram of the nematic order reconstruction phenomenon, following the biaxiality evolution inside the cell as a function of the (E, θ_U) pairs, a prohibitive task if performed on uniformly discretized domains. Our results show that intense electrical and mechanical stresses induce strong distortions of the texture which can be relaxed by growing biaxiality, ending with the coexistence of bulk and surface order reconstruction transitions in a bi-lobed region of the phase diagram. The evolution of the s_3 **Q**-tensor eigenvalue puts in evidence that textures can relax the electrical and mechanical stresses differently just underneath the upper boundary surface: the low energy side lobe includes textures which in such region have a layer where the biaxial evolution is mediated by a metastable uniaxial state; on the contrary, textures mapped within the high energy side lobe present a stable evolution from second to first order transition.

References

[1] de Gennes P G and Prost J 1993 *The Physics of Liquid Crystals* (Oxford: Clarendon Press)
[2] Barberi R, Ciuchi F, Durand G, Iovane M, Sikharulidze D, Sonnet A and Virga E G 2004 *Eur Phys J* E **13** 61–71
[3] Amoddeo A, Barberi R and Lombardo G 2012 *Phys Rev* E **85** 061705-10
[4] Amoddeo A, Barberi R and Lombardo G 2010 *Comput Math Appl* **60** 2239–52
[5] Amoddeo A, Barberi R and Lombardo G 2011 *Liq Cryst* **38** 93-103
[6] Amoddeo A, Barberi R and Lombardo G 2013 *Liq Cryst* **40** 799-809
[7] Virga E G 1994 *Variational Theories for Liquid Crystals* (London: Chapman and Hall)
[8] Sonnet A M, Maffettone P and Virga E G 2004 *J Non-Newton Fluid* **119** 51-9
[9] Sonnet A M and Virga E G 2001 *Phys Rev* E **64** 031705-10
[10] Beckett G, Mackenzie J A, Ramage A and Sloan D M 2001 *J Comput Phys* **167** 372-92